2006

Performance Analysis of a Miniature-Scale Vapor Compression System for Electronics Cooling: Bread Board Setup

Suwat Trutassanawin
Purdue University

Lorenzo Cremaschi
Purdue University

Eckhard A. Groll
Purdue University

Suresh V. Garimella
Purdue University, sureshg@purdue.edu

PERFORMANCE ANALYSIS OF A MINIATURE-SCALE VAPOR COMPRESSION SYSTEM FOR ELECTRONICS COOLING: BREAD BOARD SETUP

Suwat Trutassanawin*, Lorenzo Cremaschi, Eckhard A. Groll, and Suresh V. Garimella

Purdue University
School of Mechanical Engineering
Ray W. Herrick Laboratories
West Lafayette, Indiana, USA

*Corresponding Author: (765) 495-7515; e-mail: strutas1@purdue.edu

ABSTRACT

A Miniature-Scale vapor compression Refrigeration System (MSRS) was developed and experimentally investigated for electronics cooling. The system consists of four main components: a micro-channel cold plate evaporator-heat spreader, a compressor, a micro-channel condenser, and an expansion device. Experimental results obtained with the bread board system demonstrate the feasibility of applying a miniature-scale refrigeration system in cooling compact electronic devices. Moreover, the performance of each component and of the overall system were quantified and used to improve the efficiencies of components and system. The cooling capacity of the investigated system varied from 121 to 268 W, with a COP of 2.8 to 4.7, at pressure ratios of 1.9 to 3.2. The effectiveness of the condenser ranged from 52 to 77%, while a thermal resistance between 0.60 and 0.77 ^{o}C-cm^2/W was achieved at the evaporator. The evaporator-heat spreader thermal resistance is defined as the ratio of the temperature difference between the chip surface and the refrigerant evaporator to the evaporator heat transfer rate. The overall system thermal resistance, defined as the ratio of the temperature difference between the chip surface and the condenser air inlet, varied from 0.04 to 0.18 ^{o}C-cm^2/W. An overall second-law efficiency ranging from 33 and 52% was obtained, using a commercially available small-scale compressor. The measured overall isentropic efficiency was between 25 and 60%.

1. INTRODUCTION

As the number of transistors in integrated circuits has rapidly increased to provide more computational and functional capabilities, removing the heat generated from the electronic chips has become a critical challenge in designing compact and portable electronics devices. According to the International Technology Roadmap for Semiconductors (2003), the heat dissipation rate from a single chip package is expected to reach about 120 W and up to 220 W for a cost-performance and a high-performance single-chip packaging technology, respectively. In the meantime, the junction temperature must be maintained below 85 °C even if the ambient temperature is as high as 45 °C. Numerous alternative cooling approaches, included heat pipes, liquid immersion, jet impingement and sprays, thermoelectric, and refrigeration, have been investigated to handle the high heat dissipation rate and low junction temperature requirements and the conventional air-heat sink cooling system techniques are no longer expected to meet these requirements. A small-scale vapor compression refrigeration is one of the available approaches that can operate in high ambient temperature, and even result in negative overall system thermal resistance; that is, the vapor compression refrigeration system can provide cooling even if the chip surface temperature is lower than the ambient temperature.

The present work aims to develop a bread board miniature-scale vapor compression refrigeration system (MSRS) for electronics cooling at high heat dissipation rates. The experimental results from the bread board system were analyzed to identify each component and the overall system performances.

2. LITERATURE REVIEW

Only a few studies in the literature have investigated refrigeration systems for electronics cooling: Scott (1974), Peeples (2001), Maveety et al. (2002), Phelan and Swanson (2004), and Suman et al. (2004). The detailed of the previous studies are summarized in Trutassanawin et al. (2006). Miniature-scale refrigeration systems for electronics cooling have not been widely studied, especially by means of experimental investigation. There is also a lack of information regarding the performance of each individual component as well as a careful analysis of the energy losses in small refrigeration systems for electronics cooling applications. The present experimental investigation involves the design, construction, and testing of a miniature-scale refrigeration system (MSRS) for electronics cooling. An analysis of the results is undertaken to identify the irreversibility and the performance of the individual components as well as to demonstrate the overall performance of the small-scale refrigeration system for electronics cooling applications.

3. BREAD BOARD SETUP

A schematic diagram of the bread board system is shown in Figure 1. The system consists of five main components: a copper block to simulate the heat from the chip, a cold plate microchannel evaporator, a small-scale compressor, a microchannel condenser, and an expansion device. The cold plate evaporator and the condenser were specially designed and prototyped to fit into the space available in a personal desktop computer while the compressor and the expansion device were selected from commercially available products in the refrigeration industry. Three vertical-axial thermocouples, and two 200 W-cartridge heaters were inserted into the copper block. The cold plate evaporator included a microchannel heat exchanger integrated with a heat spreader, which distributes the heat from the small chip surface to the large heat exchanger surface. A thermally conductive paste with thermal resistance of 0.029 °C-cm^2/W was applied between the non-soldered surfaces to reduce the thermal resistance across gaps. A manual needle valve was used as the expansion device and a small-scale hermetic reciprocating R-134a compressor was used in the experimental setup. The compressor was originally designed for small-scale refrigerator applications, e.g., as used in hotel mini-bar refrigerators, and two cooling fans were used to prevent overheating of the compressor. A sight glass was used to verify the refrigerant subcooling at the condenser outlet and a filter-drier was installed in the liquid line to absorb moisture and block particles in the refrigerant flow. A hermetic coalescent oil separator was located at the discharge line to re-circulate most of the lubrication oil to the compressor suction line. The oil separator was bypassed when the reciprocating compressor was used at the condenser air inlet temperature of 35 °C in order to run the tests without the oil separator. Another sight glass was installed in the suction line to verify that there was no liquid flow to the compressor. Moreover, a suction line accumulator was placed between the sight glass and the inlet of the compressor to guarantee that only refrigerant vapor flowed to the compressor. Figure 2 shows the five main components of the system: (a) the DC reciprocating compressor; (b) the microchannel condenser; (c) the needle valve expansion device; (d) the microchannel evaporator and the copper heater block.

The compressor was a variable speed DC motor-driven reciprocating compressor. The compressor cooling capacity ranges from 143 to 221 W, the COP from 2.04 to 2.65, and the power consumption is from 66 to 104 W at the design operating conditions of ambient temperature of 55°C, suction gas temperature of 32°C, and liquid temperature at the condenser outlet of 32°C.

To simulate the heat dissipation from the CPU, a copper block with two imbedded cartridge heaters was used. The copper block had dimensions of 19 × 19 × 19 mm^3. The two cartridge heaters were mounted into the base underneath the copper block and controlled using a variable transformer. They provided up to 400 W of input power. A prototype cold plate evaporator, a copper microchannel heat exchanger, with 34 rectangular channels and a hydraulic diameter of 0.48 mm was used in the experimental setup. An integrated copper heat spreader with a thickness of 2.5 mm was soldered to the copper cold plate evaporator. The thermally conductive paste was only applied between the copper block-heat spreader interfaces since the heat spreader was soldered to the cold plate evaporator.

The expansion device was a hand-operated needle metering valve with a vernier handle for easy reading of the number of turns. The orifice nominal diameter of the valve was 0.19 mm and the length was of 17.55 mm. The flow coefficient of the orifice (for water) ranged from 0.001 to 0.004 corresponding to 4 to 10 turns, at 20°C.

A microchannel condenser with an estimated heat rejection capacity of 225 W was used in the system. The overall dimensions of the condenser were 25 × 180 × 45 mm^3, which is appropriate for installation in a 1-U rack. The condenser had 20 rectangular microchannels. Each microchannel had a hydraulic diameter of 0.43 mm. The microchannel tube length was 921 mm. The condenser consisted of five passes of microchannel tubes. The fin type was a louvered fin and the fin density was 16 fins per inch. The vapor compression system with oil separator was charged with 145 g of R-134a refrigerant, whereas the system without oil separator was charged with 125 g.

A small wind tunnel, shown schematically in Figure 3, was used to measure the heat rejected by the refrigerant to the air flow across the condenser. The wind tunnel was approximately 4.2 m in length. A pre-heater, the condenser, a nozzle, a condenser fan, and air-side instrumentation were mounted inside the duct. The pre-heater was installed at 0.15 m from the inlet air duct to control the inlet air temperature and the condenser was installed at 1.37 m downstream of the pre-heater. The DC 12V fan provided a maximum air flow rate of 200 CFM and had a maximum power input of 43.2 W. The condenser fan was installed downstream of the heat exchanger to provide sufficient air flow rate across the condenser and to overcome the pressure drop caused by the instrumentation pressure drop in the wind tunnel. All components and instrumentation were installed in the wind tunnel according to ANSI/ASHRAE Standard 41.2-1987. The refrigerant pipe, air duct, and copper block were well insulated to reduce heat losses to the ambient air.

Thermocouples and pressure transducers were installed on the refrigerant side at the inlet and outlet of the compressor, condenser, expansion device, and cold plate evaporator to determine the refrigerant state points. All temperature measurements were performed with T-Type, copper-constantan thermocouples, which were probe-type or wire-type. Their accuracy was ±0.5°C. The low-side refrigerant absolute pressure transducers ranged from 0 to 1724 kPa (0 to 250 psig) and the high-side absolute pressure transducer ranged from 0 to 3447 kPa (0 to 500 psig). The absolute pressure transducer had an accuracy of ±0.13 % of full scale. A Coriolis mass flow meter and a remote electronic unit were used to measure the refrigerant mass flow rate and they were installed in the liquid line of the system between the condenser outlet and the expansion device. The mass flow meter had a nominal range of 0 to 16 g/s and its accuracy was ±3.2 % for flow rates from 0.5 to 3 g/s. The compressor power consumption was measured by a DC power meter, which was installed before the compressor controller. The power input to the cartridge heaters in the copper block was measured by an AC power meter while the heat input to the evaporator through the copper block was determined based on an heat conduction analysis in the copper block and from the three vertical-axial temperature measurements. One more thermocouple was inserted into a groove that was cut from one side to the center to measure the surface temperature at the bottom of the heat spreader. This thermocouple was used to calculate the cold plate evaporator-heat spreader thermal resistance without the thermal resistance of the thermal conductive paste. T-Type thermocouples were installed in the copper block and at the bottom surface of the heat spreader as shown in Figure 4.

A humidity sensor was installed at the inlet of the wind tunnel, while the preheater was installed at 15 cm downstream of the duct inlet. Ten thermocouples were uniformly distributed at 13 cm upstream of the condenser, and fifteen thermocouples were uniformly distributed at 23 cm downstream of the condenser. The dimensions of the air duct rectangular cross section between the inlet and outlet thermocouples were 19 × 5 cm^2. Four inlet pressure taps were installed 5 cm upstream of the inlet thermocouple grid and four outlet pressure traps were installed 5 cm downstream of the outlet thermocouple grid, which were connected to a differential pressure transducer. The condenser air-side pressure drop was measured by a differential pressure transducer with a range from 0 to 125 Pa (0-0.5 inch H_2O) and an accuracy to within ±1.0 % of full scale. The air flow rate over the condenser was measured using a nozzle with a throat diameter of 38.1 mm and a nozzle inlet diameter of 101.6 mm. It was installed in the air duct that has the same inner diameter. The nozzle was placed at a distance 188 cm downstream of the condenser. Six thermocouples were installed 7 cm upstream of the nozzle location to obtain an average temperature for calculating the air density. Another differential pressure transducer with a range from 0 to 125 Pa (0-0.5 inch H_2O) and an accuracy to within ±1.0 % of full scale was used to measure the air-side pressure drop across the nozzle to calculate the air flow rate.

A data acquisition system was used in combination with a personal computer to collect and record all measured data at twenty-second time intervals. During the system run time, the outputs were plotted and displayed on the computer screen. This allowed the operator to adjust the control variables of the MSRS and monitored the outputs to reach the test set points. A display of the real time measurements was also used to indicate steady state operating conditions.

The test procedure were as follows: (a) The data acquisition system and the instrumentations were turned on; (b) the condenser fan and pre-heater were set to achieve the specific air flow rate and air inlet temperature, respectively; (c) the compressor and the copper block heater were turned on and adjusted to the specific compressor speed and heat flux input; (d) the manual metering valve was opened to achieve a degree of superheat between 3 and 10°C, while the subcooling temperature was set by the amount of refrigerant charge in the system; (e) the refrigerant was charged into the system only one time at the beginning of the test series to guarantee enough degree of subcooling from 3 to 15°C, for all operating conditions; and (f) the measured output signals of the sensors were converted, recorded and stored in the computer once steady-state operating conditions were achieved.

4. DATA REDUCTION

This section describes the methodology by which the experimental data were used to calculate the performance of the system and of the MSRS components. The calculated performance parameters are the chip heat dissipation rate, the evaporator-heat spreader thermal resistance, the system COP, and the overall system thermal resistance.

The heat dissipation rate from the copper block to the cold plate evaporator was calculated from the axial heat conduction in the copper block according to:

$$Q_{CPU} = \frac{k_{copper} A_c}{L_{c1-chip}} \left(T_{c1} - T_{chip,surface} \right) \tag{1}$$

where T_{c1} is the temperature at the top position in the copper block, $T_{chip,surface}$ is the chip surface temperature obtained by linear extrapolation from three thermocouples in the copper block, and $L_{c1-chip}$ is the distance between the two thermocouples as shown in Figure 4. The cooling capacity of the refrigeration system was calculated by multiplying the refrigerant mass flow rate with the refrigerant enthalpy difference across the evaporator:

$$Q_{evap,r} = \dot{m}_r \left(h_{evap,o} - h_{evap,i} \right) \tag{2}$$

From the measurements of the refrigerant outlet pressure and temperature in the single-phase superheat region, the outlet evaporator enthalpy was computed using Engineering Equation Solver (EES) software (2005). The evaporator inlet enthalpy was obtained by assuming an isenthalpic process across the expansion device. The inlet enthalpy of the expansion device was determined using EES from the measurements of the pressure and temperature in the single-phase subcooled region.

The performance of the system was characterized by the Coefficient of Performance (COP) of the overall system according to the following definitions:

$$COP_{MSRS} = \frac{Q_{evap,r}}{W_{elec}} \tag{3}$$

where the overall system work, W_{elec}, including the power consumption of the compressor, condenser fan, and compressor cooling fans:

$$W_{elec} = W_{comp,elec} + W_{cond,fan} + W_{comp,fans} \tag{4}$$

For the cold plate evaporator heat spreader, the conventional definition of heat exchanger effectiveness was not applicable because the heat was transferred from the chip to the refrigerant and only one fluid is present in the heat exchanger. Therefore, the cold plate evaporator thermal resistance was used to characterize the performance of the cold plate evaporator:

$$R_{th,evap} = \frac{T_{HS,bottom} - T_{evap}}{Q_{evap,r}} \quad (5)$$

If the cold plate evaporator thermal resistance is low, then either the bottom heat spreader temperature is close to the refrigerant evaporator temperature (low temperature difference) or the chip heat dissipation rate is quite high. In both cases, a lower the thermal resistance leads to a higher performance of the cold plate evaporator. The overall system thermal resistance was defined as the ratio of the difference between the bottom heat spreader surface and condenser air inlet temperatures to the chip dissipation rate:

$$R_{th,sys} = \frac{T_{HS,bottom} - T_{air,i}}{Q_{CPU}} \quad (6)$$

As for the evaporator thermal resistance, if the overall system thermal resistance is low, then either the bottom heat spreader temperature is close to the condenser air inlet temperature or the chip heat dissipation rate is high. Therefore, the lower the overall system thermal resistance, the higher is the performance of the MSRS. Eventually, the overall system thermal resistance can become negative, which occurs when the bottom heat spreader temperature is lower than the condenser air inlet temperature. A negative overall system thermal resistance is achieved only if a refrigeration system is used because the system continues to provide cooling even if the chip surface temperature is lower than the surrounding ambient air temperature. In this case, the refrigeration system behaves like a small-scale heat pump that extracts heat from the CPU, transfers heat away from the hot spots, and rejects heat to the ambient air. This feature is particularly attractive for thermal management of compact and integrated electronic devices inside desktop and laptop computers. As opposed to MSRS, a conventional air heat sink cooling system always has positive overall system thermal resistance, which means that the chip surface temperature will always be higher than the surrounding air temperature.

5. EXPERIMENTAL RESULTS

A bread board Miniature-Scale Refrigeration System (MSRS) for electronics cooling was tested at various operating conditions. An experimental parametric study was performed by varying the condenser air flow rate, the condenser air inlet temperature, the superheat temperature, and the chip heat dissipation rate. The condenser air flow rate was controlled by varying the voltage or input power to the condenser fan and the condenser air inlet temperature was varied by changing the power input to the pre-heater in the wind tunnel. The superheat temperature was controlled via the manual needle valve and the chip heat dissipation rate was regulated by the input power to the cartridge heaters inserted into the copper block. In addition, refrigerant R-134a was charged into the MSRS to have enough degree of subcooling at the condenser outlet from 3 to 15 °C for the entire ranges of the operating conditions.

5.1 Experimental Results for the Components

The volumetric and overall isentropic efficiencies of the compressor range from 58-73 % and 43-57 %, respectively as shown in Figure 5. This means that both compressor efficiencies are generally lower than the expected values of small-scale compressors because the compressor used in the experiments was operated outside of its design operating conditions. The compressor efficiencies when using the oil separator are lower than that of the compressor without oil separator. This is because some refrigerant flows back to the suction line with the return oil when using the oil separator. As expected, the volumetric efficiency increases with a decrease of the pressure ratio. However, the overall isentropic efficiency increases with an increase of the pressure ratio since the compressor was operated at off-design conditions. During the experiments, the pressure ratios were lower than the design pressure ratio for the specific compressor (the design pressure ratio ranges from 4.5 to 15.6). The pressure ratio ranged from 1.9 to 3.1 and the refrigerant mass flow rate was from 1.9 to 2.3 g/s. The total electrical power consumption of the compressor and the compressor cooling fans was between 39 and 45 W depending on the operating conditions. The compressor shell average surface temperature ranged from 34 to 44 °C.

The reciprocating compressor uses a flexible reed valve, acting like a spring, which is chosen to operate at the designed suction pressure. If the suction pressure is higher than the design pressure, then the pressure drop across the suction valve might change and the amount of gas leaking through the suction valve is expected to be higher. Moreover, the higher the suction pressure, the larger is the refrigerant vapor density. Thus, the refrigerant vapor density at the tested condition is larger than that at the design condition. As a result, the pressure drop owing to the

re-expansion of the vapor refrigerant at the test condition is higher than that of the design condition because there is more refrigerant vapor left in the clearance volume of the compressor. In addition, the heat loss from the compressor shell to the surroundings of the reciprocating compressor is also higher because the compressor has more surface area, that is, it is an oversized compressor. Since the compressor was run at off-design conditions, the compressor efficiencies were quite low. In general, overall isentropic efficiencies are expected to be between 50-70 % for small and medium-scale compressors with 3 to 10 kW cooling capacity (Groll and Braun, 2004). A new compact design of the compressor is necessary for this application. The compressor must have a mass flow rate ranging from 0.8 to 2.0 g/s, a pressure ratio from 1.8 to 3.2, and a refrigerant evaporation temperature from 10 to 25 °C.

The energy balance of the microchannel condenser between the air and refrigerant sides was within ±10 % with a standard deviation of 8.9 %. The discrepancy in the energy balance of the condenser was mostly due to inaccuracies in determining the air volume flow rates. The condenser heat rejection rate varied from 130 to 260 W and the condenser effectiveness ranged from 46 to 77 %. The air flow rates varied from 9.4×10^{-3} to 14.2×10^{-3} m^3/s (20 to 30 CFM) and the condenser air inlet temperatures were held at 25 and 35 °C. During the experiments, the refrigerant condensing temperatures were measured to be between 44 and 61 °C. The energy balance of the cold plate evaporator was computed between the chip heat dissipation rate and the refrigerant cooling capacity and was within ±15 % with a standard deviation of 8.9 %. Generally, the measured refrigerant side cooling capacity was lower than the measured heat transfer rate from the copper block. The reasons for this consistent discrepancy include heat losses from the copper block/heat spreader through the insulation to the ambient air. Fluctuations in the discrepancies of the evaporator energy balances were due to measurement uncertainty. The degree of superheat was between 3 and 6 °C, the condenser air inlet temperature was approximately 25 °C, and the air flow rate ranged from 9.4×10^{-3} to 16.5×10^{-3} m^3/s (20 to 30 CFM). The evaporator-heat spreader thermal resistance was employed to estimate the efficiency of the cold plate evaporators as shown in Figure 6 and ranged from 0.2 to 0.7 °C-cm^2/W. The system could dissipate a chip heat transfer rate from 176 to 226 W and was able to maintain the chip surface temperature between 34 and 53 °C (while the refrigerant evaporator temperature ranged from 14 to 25 °C).

5.2 System Performance

The system COP and the overall system thermal resistance were used to evaluate and assess the performance of the system. The system COP as a function of the pressure ratio is shown in Figure 7. The measured COP was between 2.6 and 3.7. The sensitivity of the cooling COP is affected more by the total electrical power consumption of the MSRS than the cooling capacity of the system. The overall system thermal resistance at condenser air inlet temperature of 25 and 35°C are displayed in Figure 8 as a function of the chip surface temperature. The miniature-scale refrigeration system has an overall system thermal resistance between 5.5×10^{-3} and 0.11 °C/W (0.02-0.40 °C-cm^2/W) and is able to maintain a relatively low chip surface temperature (from 34 to 70 °C) together with a high heat dissipation rate (from 150 and 210 W). In all tests, the chip surface temperature was always lower than the maximum allowable temperature of 85 °C.

6. CONCLUSIONS

A bread board miniature-scale vapor compression refrigeration system (MSRS) using R-134a as the refrigerant was designed, built, and tested. A commercially available small-scale compressor was installed in the MSRS. From an extensive experimental investigation, the main energy losses of the MSRS were highlighted. The most significant losses occurred in the compressor while the condenser and the evaporator performed to specifications. The overall isentropic efficiencies range from 43-57 %. The condenser effectiveness ranged from 46 to 77 % and the evaporator-heat spreader thermal resistance ranged from 0.2 to 0.7 °C-cm^2/W. The experimental results showed that the system was able to dissipate CPU heat fluxes of approximately 40-75 W/cm^2 and keep the junction temperature below 85°C for a chip size of 1.9 cm^2. The MSRS system has an overall system thermal resistance between 0.02 to 0.42 °C-cm^2/W, the chip heat dissipation rate was between 176 and 226 W and the chip surface temperature was between 34-53 °C. However, if a miniature-scale vapor compression system is used in electronics cooling applications, the efficiency and reliability of the compressor should be considered carefully. A new compressor design for electronics cooling should be targeted in future work. The novel compressor needs to fit within 45 mm

height (1-U rack), it has to be thermodynamically efficient for the operating conditions of the current application, and it has to guarantee good reliability for continuous running inside desktop computers.

NOMENCLATURE

A	Area (m)	(m^2)	**Subscripts**	
			air	Air
k	Thermal conductivity	(W/m-K)	$chip$	Chip
			$elec$	Electric
L	Length		$evap$	Evaporator
$\dot{m}$	Mass flow rate	(g/s)	HS	Heat spreader
$\dot{Q}$	Heat transfer rate	(W)	i	Inlet
R	Thermal resistance	(°C/W)	o	Overall, outlet
T	Temperature	(°C)	$r, refrig$	Refrigerant
$\dot{W}$	Power consumption	(W)		

REFERENCES

Maveety, J.G., et al., 2002, "Thermal Management for Electronics Cooling Using a Miniature Compressor," International Microelectronics and Packaging Society (IMAPS), Denver, CO.

Peeples, J.W., 2001 "Vapor Compression Cooling for High Performance Applications," Electronics Cooling, Vol. 7, pp. 16-24.

Phelan, P.E., and Swanson, J., 2004 "Designing a Mesoscale Vapor-Compression Refrigerator for Cooling High-Power Microelectronic," Inter Society Conference on Thermal & Themomechanical Phenomena in Electronic Systems (I-THERM), Las Vegas, NV, June 1-4, pp. 218-223.

Scott, A.W., 1974, Cooling of Electronic Equipment, John Wiley and Sons, pp. 204-227.

Schmidt, R.R., and Notohardjono, B.D., 2002, High-End Server Low-Temperature Cooling, IBM Journal Research and Development, Vol. 46, pp. 739-751.

Suman, S., Fedorov, A., and Joshi, Y., 2004, "Cryogenic/Sub-Ambient Cooling of Electronics: Revisited," Inter Society Conference on Thermal & Themomechanical Phenomena in Electronic Systems (I-THERM), Las Vegas, NV, June 1-4, pp. 224-231.

Trutassanawin, S., Groll, A.E., Garimella, V.S., and Cremaschi, L., 2006, "Experimental Investigation of a Miniature-Scale Refrigeration System for Electronics Cooling," IEEE Transaction on Components and Packaging Technologies, (in press).

ACKNOWLEDGEMENT

The financial support for this work from the Cooling Technologies Research Center (CTRC) at Purdue University is greatly appreciated as are discussions and suggestions from members of the CTRC.

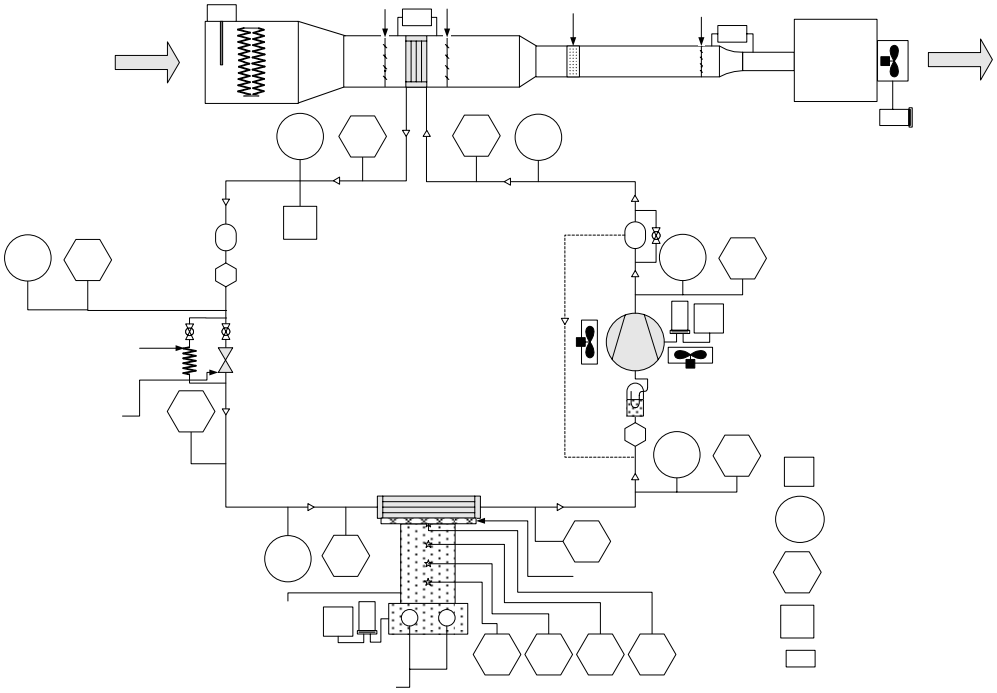

Figure 1: Schematic diagram of bread board MSRS.

(a)

(b)

(c)

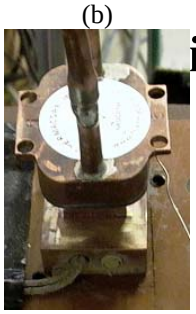

(d)

Figure 2: Components of MSRS for electronics cooling: (a) Reciprocating compressor; (b) Microchannel condenser; (c) Needle valve and capillary tube; (d) Microchannel evaporator – copper heater block.

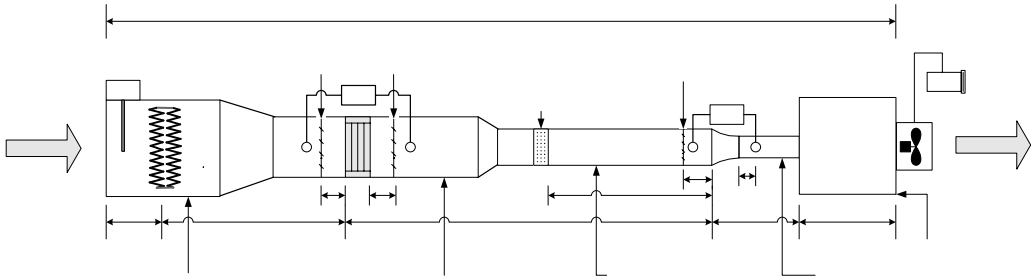

Figure 3**:** Wind tunnel to measure air flow rate and condenser heat rejection rate.

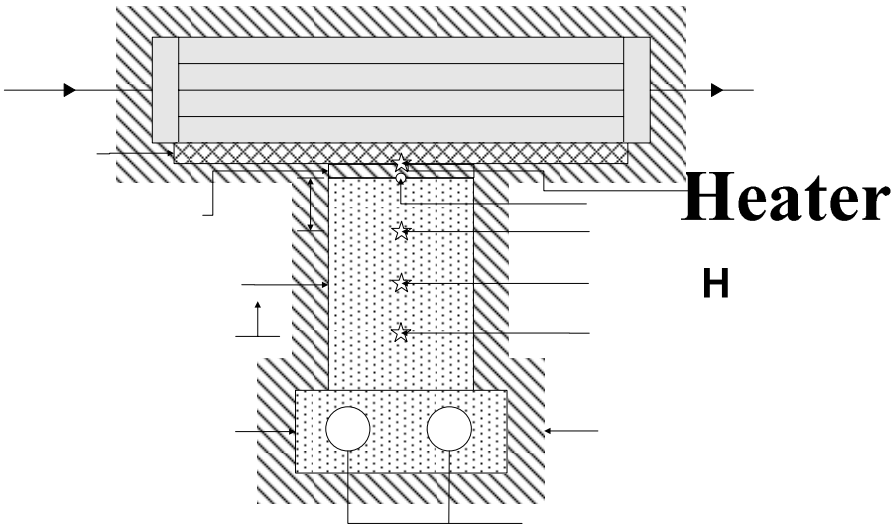

Figure 4: Schematic diagram of cold plate microchannel evaporator and copper cold block.

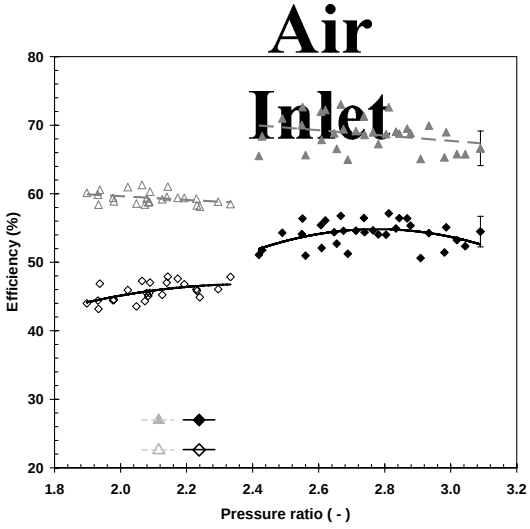

Figure 5: Compressor volumetric and overall isentropic efficiencies versus pressure ratio.

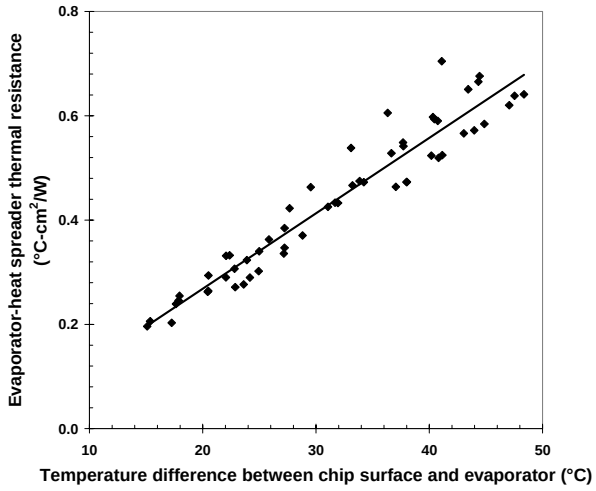

Figure 6: Evaporator-heat spreader thermal resistance versus temperature difference between chip surface and evaporator.

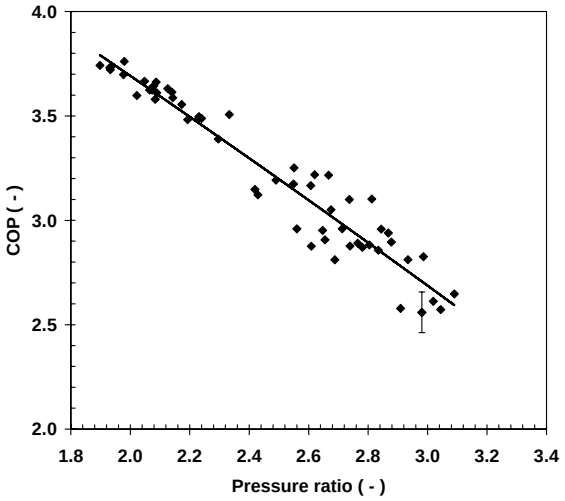

Figure 7: Coefficient of performance versus refrigerant pressure ratio.

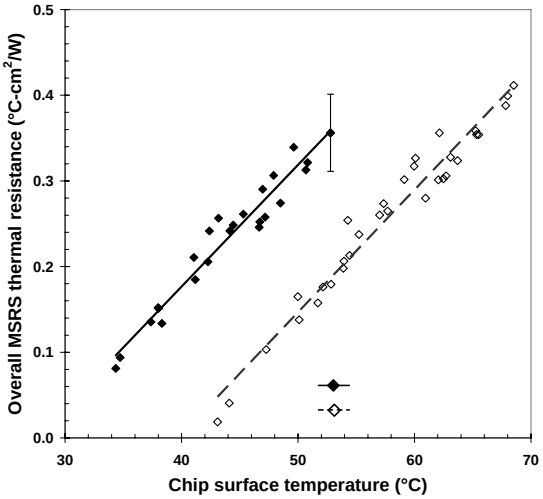

Figure 8: Overall system thermal resistance versus chip surface temperature.